

## CHAPTER 11

### ANOMALOUS DYNAMICS OF POLYMER FILMS

Ophelia K. C. Tsui

*Department of Physics, Boston University  
Boston, MA 02215, U.S.A.  
E-mail: okctsui@bu.edu*

This chapter reviews the recent experiments involving the dynamics of polymer films with thickness comparable to the gyration radius of the polymer, which overwhelmingly show that their glass transition temperature,  $T_g$ , depends on the film thickness and can sometimes differ significantly from that of the bulk. The greatest mystery is the onset film thickness of this phenomenon being  $\sim 50$  nm, much larger than the typical cooperativity size ( $\sim 3$  nm) of glass transition. While the sliding chain model [De Gennes, *Eur. Phys. J. E* (2000)] can qualitatively explain the results of the high molecular weight ( $M_w$ ) freely-standing films, it fails to account for those of the low- $M_w$  freely-standing films and the supported films. For the latter two, at least two theories, *i.e.*, the percolation theory [Long *et al.*, *ibid* (2001)] and surface capillary wave theory [Herminghaus *et al.*, *ibid* (2001)] have been proposed that can account for the observed thickness dependence of thin film  $T_g$ . However, experimental data available at this time do not allow the theories to be distinguished. We briefly outline the physical ideas of these theories, and delineate how dynamical measurements of nanometer thick films may provide important insights about the problem.

#### 1. Introduction

A fundamental understanding of the dynamical and mechanical properties of polymer thin films is important in many applications

including organic light emitting devices, protective encapsulations in microelectronics, and lubricant coatings, *etc.* There has been mounting evidence over the past two decades showing that the properties we know well about polymers in bulk often do not apply when they are made into thin films, especially when the film thickness is comparable to the gyration radius of the polymer (typically 2 to 50 nm).<sup>1-13</sup> Nonetheless, a large number of these observations remain unexplained, and understanding the origins of the anomalous dynamics of polymer films has become one of the most challenging problems of contemporary polymer physics. The purpose of this chapter is to give a brief account of this rapidly evolving field of research. At the time when this chapter is written, several excellent reviews on the subject have been published.<sup>1-4</sup> Due to limitation of space, the selection of materials in this review may be skewed to the author's personal interest. The readers are referred to the previous reviews<sup>1-4</sup> for a more thorough view about the subject.

## 2. Experimental Observations on the $T_g$ of Polymer Films

The study of dynamics of glass forming liquids under confinement at the nanoscale was first carried out by Jackson and McKenna<sup>14</sup>. In that work, a depression of  $T_g$  of 8.8K was found in *o*-terphenyl confined in

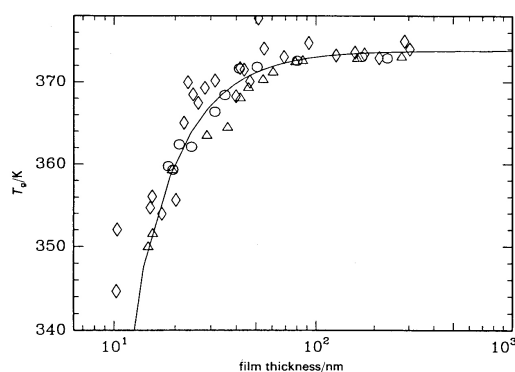


Fig. 1.  $T_g$  (K) vs. film thickness (nm) of PS supported on silicon with different molecular weights,  $M_w$  of 120K (circles), 500.8K (triangles) and 2,900K g/mol (diamonds). The solid line is the best fit to Eq. 1. Data by Keddie et al. reproduced from Ref. 19 (copyright RSC Publishing).

controlled pore glasses treated with hexamethyldisilazane and have an average pore diameter of 8.5 nm. Soon afterwards, Reiter found that polystyrene (PS) films with thickness  $< 8$  nm supported by a glass substrate could dewet at temperatures below the bulk  $T_g$ , providing evidence that the  $T_g$  of these films can be smaller than the bulk value.<sup>15-17</sup> Keddie and coworkers<sup>18,19</sup> were the first to systematically measure the  $T_g$  of polymer films as a function of the film thickness,  $h$ . Figure 1 shows their result on PS supported by silicon. The most surprising finding from this result is the absence of any dependence on the molecular weight,  $M_w$ , of the polymer (120K to 2900K g/mol) in the  $T_g$  vs.  $h$  dependence. The data for  $T_g(h)$  was found to empirically fit the following:

$$T_g(h) = T_g(\infty)[1 - (\delta/h)^v], \quad (1)$$

where  $\delta$  and  $v$  are fitting parameters with values 3.2 nm and 1.8, respectively, found by Keddie *et al.*<sup>18,19</sup> for PS on silicon. These authors postulated that Eq. 1 could arise from a low-density, highly mobile layer at the free surface of the film having an intrinsic thickness of  $\delta$  that diverges like  $(1 - T/T_g(\infty))^{-1/v}$  as the temperature approaches the bulk  $T_g$  from below. On the other hand, qualitatively different behaviors were reported by them in the same papers.<sup>18,19</sup> It was observed that the  $T_g$  of poly(methyl methacrylate) (PMMA) films could increase or decrease with decreasing film thickness depending on the substrate material and surface condition as illustrated in Fig. 2. Specifically, PMMA films on gold coated silicon showed a decrease in  $T_g$  with decreasing film thickness, but those deposited on silicon covered by a native oxide layer showed an increase in  $T_g$  with decreasing film thickness. Later, other supported polymer films were also found to demonstrate an increase in  $T_g$  with decreasing film thickness, such as poly(2-vinyl pyridine) on acid-cleaned silicon oxide.<sup>20</sup>

A layered model is one of the earliest models proposed to explain these observations,<sup>18-25</sup> and by far the most accepted for the thickness dependence of the  $T_g$  of polymer films. The model presupposes that the molecular motions near the polymer-air interface are much faster than those in the bulk polymer, which can be due to segregation of chain ends

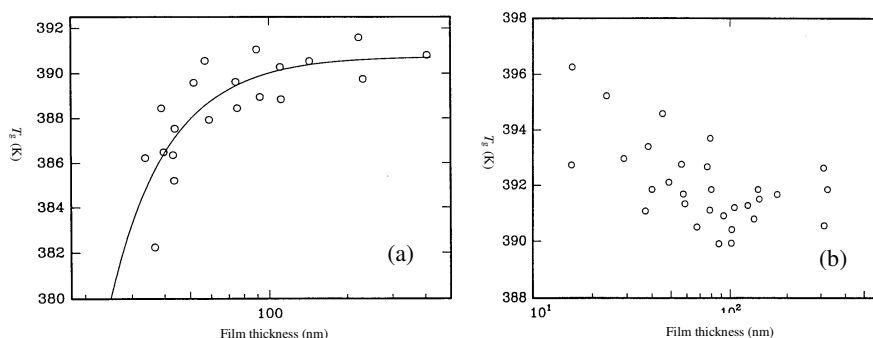


Fig. 2.  $T_g$  (K) vs film thickness (nm) of PMMA films deposited on (a) gold coated silicon and (b) silicon covered by a native oxide layer. Data by Keddie *et al.*, reproduced from Ref. 19 (copyright RSC Publishing).

to the surface<sup>24,26</sup> or a reduction in the chain entanglement near the polymer free surface.<sup>24,27</sup> On the other hand, the molecular motions at the polymer-substrate interface can be faster or slower than the polymer motions in bulk depending on whether the polymer-substrate interactions are sufficiently weak or strong, respectively. The  $T_g$  of a film is a result of the interplay between the effects of the two interfaces. The x-ray photoelectron spectroscopic (TDXPS) and angle-dependent XPS measurements of Kajiyama *et al.*<sup>28</sup> on poly(styrene-*b*-methyl methacrylate) showed that the  $T_g$  of the polymer got progressively smaller than that of the bulk towards the free surface. By using fluorescence labeling, Torkelson's group<sup>29</sup> showed that the local  $T_g$  of PS was smaller than the bulk value at the free surface, but continuously approached the bulk  $T_g$  over several tens of nm into the film. Numerous computer simulation results also support this picture.<sup>30-35</sup> These findings provide important evidence to the existence of dynamical heterogeneity — which is indeed a gradient — in the film, and validates the use of the layered model.

### 2.1. Experimental Search for Enhanced Mobility at the Polymer-Air Interface

The idea that there can be a mobile layer at the free surface of a polymer has fascinated numerous researchers who have devised some most

ingenious experiments to search for its existence.<sup>22,28,29,36-50</sup> These experiments involved a large number of measurement techniques, which include angle-dependent x-ray photoelectron spectroscopy,<sup>28</sup> various kinds of atomic force microscopy (AFM),<sup>37-42</sup> near-edge x-ray absorption fine structure,<sup>43,44</sup> positron annihilation lifetime spectroscopy,<sup>22,45</sup> optical birefringence measurement,<sup>46</sup> melting of a topographic structure,<sup>49,50</sup> and local  $T_g$  probe by fluorescence labeling.<sup>29</sup> Although some of the results are conflicting, the majority holds that the mobility of PS, for which the thin film  $T_g$  shows the biggest reduction, is enhanced near the free surface. And between two conflicting results obtained by the same technique, the more recent one indicates that the surface mobility is enhanced. For AFM experiments showing a conflicting result, one can usually find attributes to the specificity of the polymer, inadequacy of the surface sensitivity of the technique and/or alternative interpretations of the results. I postpone further discussions until Sec. 5.2. For experiments involved rubbed PS, studies show that the relaxation phenomenon is rich and may not be simply related to the glass transition of the polymer.<sup>47,48</sup>

The search for an enhanced mobility surface layer is connected with the search for the origin of a reduction in the thin film  $T_g$ . In contrast, the search for the origin of an increase in the thin film  $T_g$  has not aroused nearly as much interest. It is attributable to the fact that an increase in  $T_g$  can always be ascribed to the friction between the polymer chains and the substrate. Furthermore, far more examples have been found for decreases than increases in the  $T_g$  of polymer films, which also makes the former more appealing.

## **2.2. Significance of the Polymer-Air Interface and Confinement Effect Revealed by Freely-Standing Films**

The importance of the polymer-air interface in bringing about a reduction in the  $T_g$  of a polymer film can also be perceived from the results of freely-standing films,<sup>51-57</sup> which possess two polymer-air interfaces (Fig. 3). From the measured  $T_g$  of PS freely-standing films (Fig. 4),<sup>51-55</sup> one may readily notice that the magnitude of the shift in  $T_g(h)$  is twice as large as that found in supported PS films (Fig. 1). In addition, the data

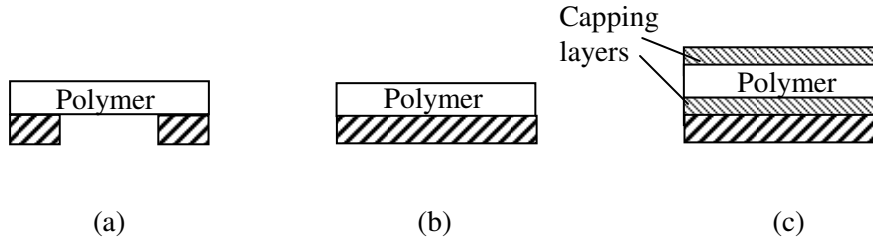


Fig. 3. Three configurations commonly employed in the study of polymer films: (a) freely-standing, (b) supported and (c) capped films. These configurations differ by the number of polymer-air and polymer-substrate interface, and allow systematic control of the effect of these two kinds of interfaces on the dynamics of polymer films.

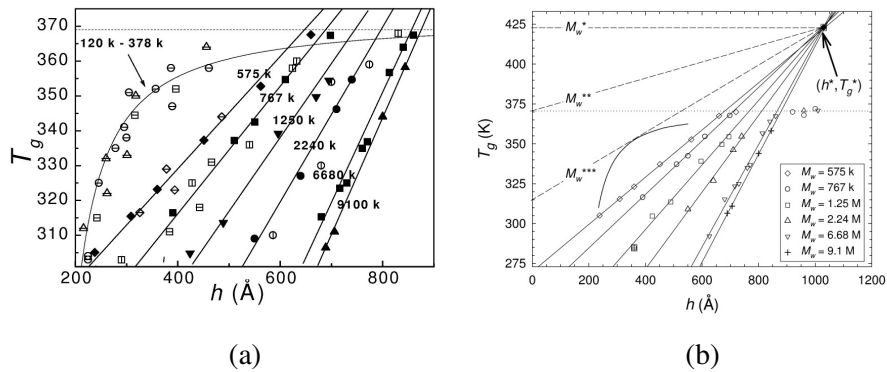


Fig. 4. (a)  $T_g$  of freely-standing PS films with  $M_w$  from 120 K to 9100 K g/mol obtained by different techniques. The solid symbols are obtained by ellipsometry. The hollow symbols are obtained by Brillouin light scattering. The solid lines are fits to the data to Eq. 2. (b) The same data shown in (a), but for  $M_w > 378$  K g/mol only. The fitted lines are extrapolated above the bulk  $T_g$  and are found to meet at a point denoted by  $(h^*, T_g^*)$  as shown. The physical meaning of the convergence at  $(h^*, T_g^*)$  is not known. (Both figures are reproduced from Ref. 4, copyright Elsevier.)

behave quite differently between the  $M_w \geq 575$  kg/mol films and the  $M_w \leq 378$  kg/mol films, as a result of which they were referred to as the high- and low- $M_w$  films, respectively. For the high- $M_w$  films,  $T_g(h)$  is equal to the bulk  $T_g$  at large film thicknesses, but starts to decrease linearly with the film thickness below some threshold thickness. From Fig. 4, as  $M_w$  decreases the threshold thickness decreases and the slope of

$T_g(h)$  below the threshold gets smaller. The fact that the shift in  $T_g(h)$  depends on the comparison between the unperturbed size of the polymer ( $\sim M_w^{1/2}$ ) and the film thickness evidences that chain confinement effect of some sort exists. For the low- $M_w$  films, on the other hand, the variation of  $T_g(h)$  is gradual, showing no  $M_w$  dependence as was found in supported films (Fig. 1). In fact, Eq. 1 that generally fits the data of supported films provides a good description of the low- $M_w$  data as well (Please see the solid, curved line in Fig. 4(a)). The fitted value of  $\delta$ , with  $\nu$  fixed at 1.8, is 7.8 nm.<sup>3</sup> It is noteworthy that this value is twice the value found for the supported films. Since freely-standing films possess twice the number of polymer-air interfaces as supported films do, this result reinforces the layered model that the reduction of  $T_g$  in polymer films is caused by a mobile layer at the polymer-air surface. As for the high- $M_w$  data (Fig. 4(a)), it was found<sup>55</sup> that the linear regression lines through the data actually extrapolate to meet at a single point,  $(h^*, T_g^*) = (103 \text{ nm}, 423 \text{ K})$  above the bulk  $T_g$  (Fig. 4(b)). This suggests that the  $T_g(h)$  of high- $M_w$  freely-standing films can be written as<sup>55</sup>:

$$T_g - T_g^* = \alpha(M_w)(h - h^*). \quad (2)$$

Empirically, 
$$\alpha(M_w) = b \ln(M_w / M_w^*), \quad (3)$$

where  $b = (0.70 \pm 0.02) \text{ K/nm}$  and  $M_w^* = (69 \pm 4) \text{ kg/mol}$ . Forrest and Dalnoki-Veress argued that the  $T_g(h)$  dependence described by Eq. 2 should yield to the low- $M_w$  behavior (i.e., the curved line in Fig. 4(a)) when the slope  $\alpha(M_w)$  is decreased to such a point that the corresponding  $T_g(h, M_w)$  line touches the low- $M_w$  curve only at a single point. This condition is illustrated by the straight line marked by  $M^{***}$  in Fig. 4(b) (the short curved line depicts a segment of the low- $M_w$  curve). The value of  $M^{***}$  thus estimated is 300 K g/mol, which agrees well with the crossover at  $M_w = 378 \text{ K g/mol}$  seen in Fig. 4(a).

Qualitatively the same results were found in freely-standing PMMA films by the Dutcher group recently<sup>56,57</sup> although the magnitude of the  $T_g$  reduction is roughly a factor of three less than that found in the PS films. It points to the importance of the specificity of the polymer on its thin

film properties, and is consistent with the lack of enhanced surface mobility often found in acrylate polymers.<sup>39,41,42</sup>

### 2.3. Effect of Chain Ends

Local enrichment of the chain ends at the free surface of a polymer has been one of the most cited origins for the surface mobile layer. The phenomenon was confirmed by Kaijiyima *et al.*<sup>38</sup> who found that the concentration of surface chain ends diminished as the  $M_w$  of the studied PS was increased and became negligibly small when the  $M_w$  is bigger than the entanglement molecular weight ( $\sim 30$  kDa). Motivated by these results, we investigated<sup>24</sup> the thickness dependence of  $T_g$  of monodispersed PS thin films with  $M_w = 13.7$  K and 550 K Da ( $M_w/M_n \leq 1.06$  for both polymers) to seek for any effect on the  $T_g(h)$  dependence due to the higher concentration of surface chain ends expected in the 13.7 kDa than the 550 kDa PS films. As seen in Fig. 5 (main panel), the measured  $T_g(h)$  demonstrate excellent fits to Eq. 1. In the inset is shown the same data normalized by the corresponding bulk  $T_g$ . Evidently, the data of both molecular weights almost overlap, indicating that the  $T_g(h)$

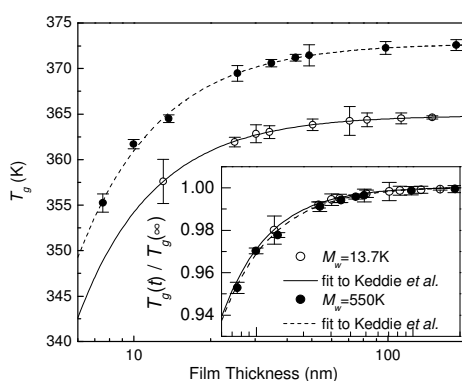


Fig. 5. (main panel)  $T_g$  vs.  $h$  for PS films with  $M_w = 550$  kDa (solid circles) and 13.7 kDa (open circles). The solid and dashed lines are fits to Eq. 1. (inset) The same data but normalized by the corresponding bulk  $T_g$  of the polymer,  $T_g(\infty)$ , determined from the fits shown in the main panel (reproduced from Ref. 24, copyright American Chemical Society.)

dependence is independent of  $M_w$  even below the entanglement molecular weight<sup>58</sup> and hence the surface chain ends cannot constitute an essential cause for the reduction of  $T_g$  in PS supported films. This result is in keeping with the simulation work of Doruker and Mattice<sup>59</sup> who found that the segmental mobility at the free surface was enhanced for

both linear and cyclic polymer chains. To investigate if there is at all any influence of the surface chain ends on the  $T_g$  of polymer films, we studied the  $M_w$  dependence (from 13.7 K to 2.3M Da) of  $T_g$  of PS films with fixed thicknesses of 15 and 50 nm, respectively.<sup>24</sup> Shown in Fig. 6 are the results plotted as  $T_g(M_w)/T_g(M_w = \infty)$  vs.  $M_w$  for the two thicknesses as well as the bulk polymer, where  $T_g(M_w = 2.3M)$  was taken to be  $T_g(M_w = \infty)$ . According to Fox and Flory (FF),<sup>60</sup>

$$T_g(M_w)/T_g(M_w = \infty) = 1 - m_0/M_w, \quad (4)$$

where  $m_0 \sim (\rho_s - \rho_e)$  with  $\rho_s$  and  $\rho_e$  being the mass density of a chain segment and chain end, respectively. For PS,  $T_g(M_w = \infty) = 373$  K and  $m_0 = 455.8$ .<sup>60</sup> As seen in Fig. 6, Eq. 4 provides fairly good fits to the data (solid lines), and the  $M_w$  dependence of  $T_g$  weakens as the film thickness decreases. The fitted value of  $m_0$  for the 15 nm films is 40% less than that of PS in bulk. A reduction in  $m_0$  may either be due to an increase in  $\rho_e$  or a decrease in  $\rho_s$ . Since the inset of Fig. 5 shows that the reduction in the  $T_g$  of a 15 nm film is only  $\sim 2\%$  of  $T_g(\infty)$ , which puts an upper limit to the possible reduction in  $\rho_s$  of the polymer under confinement in a 15 nm thickness. A 2% reduction in  $\rho_s$  would be too small to account for the 40% reduction in  $\rho_s - \rho_e$  deduced above. Therefore, the apparent reduction in  $m_0$  is most likely due to an increase in  $\rho_e$  as the film thickness is reduced. A probable explanation to this observation would

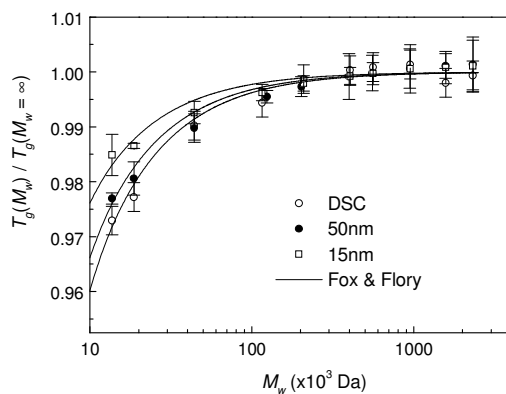


Fig. 6.  $T_g(M_w)$  normalized by the  $T_g$  at  $M_w = 2.3M$  Da as a function of  $M_w$  for samples in bulk (open circles) and in thin films with  $h = 50$  nm (solid circles) and 15 nm (open squares). Solid lines are fits to Eq. 4.

be an enhanced segregation of the chain ends to the surface as the polymer thickness decreases, resulting in a reduction in the number of chain ends remaining in the film body that ultimately determines the  $T_g$  of the film. To confirm that the change in  $T_g$  vs.  $M_w$  shown in Fig. 6 is indeed a reflection of the change in the number fraction of chain ends in the film body, we studied the  $T_g(h)$  dependence of a binary blend of 13.7 K and 550 K PS (in 1:1 wt. ratio).<sup>24</sup> For a binary blend of polymers with disparate molecular weights, Hariharan *et al.*<sup>61</sup> showed that entropic effect would drive the low- $M_w$  component to the film surface, producing a local enrichment of the low- $M_w$  component. Thus, one expects the 13.7 K constituent in the blend films to segregate to the surface. By using Fox and Flory's (FF) model, the  $T_g$  of the binary blend in bulk should be<sup>60</sup>:

$$1/T_g = 1/2[1/T_g(M_w=13.7 \text{ K}) + 1/T_g(M_w=550 \text{ K})]. \quad (5)$$

In Fig. 7 (solid line) is displayed this dependence assuming the measured  $T_g$  of the respectively monodispersed films. The measured  $T_g$ 's of the blend films are shown by solid squares. As seen, the data agree with this model line quite well for  $h > \sim 30$  nm, but approaches the  $T_g$  of the 550 K PS films when the film gets thinner. Our result strongly suggests that those chain ends segregated to the surface do not contribute to the  $T_g$  of the film, but instead only those remaining in the film body do. This reinforces our above observation that the surface chain ends are not directly related to the reduction of  $T_g$  observed in polymer films.

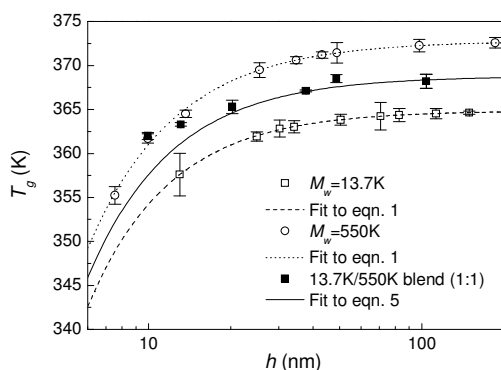


Fig. 7. Comparison between the  $T_g$  of the 13.7 K/550 K (1:1 in wt) blend films (solid squares) and that of the pure constituents reproduced from Fig. 5. The continuous lines passing through individual data sets are fits to Eq. 5.

#### 2.4. Effect of the Polymer-Substrate Interface

We have examined yet another popular perception about the thickness dependence of polymer film  $T_g$ , i.e., the amount of  $T_g$  reduction or increase of a polymer supported film depends on, respectively, how repulsive or attractive the polymer-substrate interaction is. The  $T_g$  of 33 nm thick PS ( $M_w = 96$  kDa,  $M_w/M_n = 1.04$ , bulk  $T_g = 373$  K) coated on random copolymer of PS and PMMA (P(S-*r*-MMA)) brushes with  $M_w \sim 10$  kDa,  $M_w/M_n \sim 1.1$  to 1.8 was studied as a function of the styrene fraction,  $f$ , of the brush.<sup>25</sup> The result, plotted as  $T_g$  vs.  $f$  is shown in Fig. 8. As seen, as  $f$  is decreased from 1, the  $T_g$  of the films decreases and reaches  $\sim 351$  K at  $f \sim 0.7$ , showing that the thin film  $T_g$  decreases as the polymer-substrate interaction gets more unfavorable. We examine in what way the polymer-substrate interaction energy may manifest in this effect. The transition of a liquid into a glass corresponds to a kinetic arrest of the liquid as a result of the necessity of cooperative molecular rearrangement in order for any motion (involving configurational changes) to be possible.<sup>62</sup> Because cooperativity is involved in the dynamics at the glass transition,  $T_g$  should be determined by the total

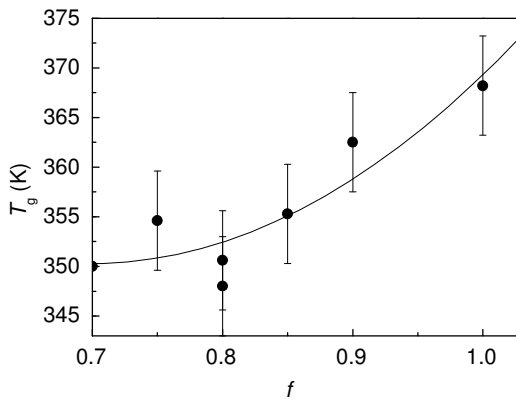


Fig. 8. The measured  $T_g$  of 33 nm thick PS films spin-coated on P(S-*r*-MMA) brushes as a function of the styrene fraction,  $f$ , of the brush (solid symbols). The solid line is a guide-to-the-eye.

energy,  $N_\xi \epsilon_a$ , required to activate all the molecules in a cooperative region to move simultaneously. By using the published data of PS with  $M_w$  similar to ours,<sup>63</sup> we estimate that  $\epsilon_a \sim 130$  Jcm<sup>-3</sup>.<sup>25</sup> To the first-order approximation, an interfacial energy of  $\gamma_{sf}$  should produce a change in

the glass transition temperature,  $\delta T_g \sim \gamma_{sf} T_g / (\epsilon_a \xi)$ , where  $\xi$  is the size of a cooperative region. Based on previous measurements of  $\gamma_{sf}$  vs.  $f$ ,<sup>64,65</sup> the change in  $\gamma_{sf}$  when  $f$  is changed by 0.3 is  $0.43 \text{ erg/cm}^2$ . Hence, to obtain the observed change of 20 K in  $T_g$  as  $f$  was decreased from 1 to 0.7,  $\xi$  would have to be  $0.6 \text{ \AA}$ , which is unphysically small. This simple estimate shows that the value of  $\gamma_{sf}$  alone does not provide sufficient ground to understand the effect of interfacial interaction on the  $T_g$  of polymer films.

At the interface between the homopolymer and the brush, the specific interactions between monomers and packing constraints would produce perturbations to the chain conformations. Consider  $(\delta T_g / \delta \rho)$ , the reduction in  $T_g$  due to a decrease in the mass density,  $\rho$ , because of the perturbation.  $(\delta T_g / \delta \rho) = (\delta T_g / \delta P)(\delta P / \delta \rho) = (\delta T_g / \delta P)(1 / \rho \kappa)$ , where, for PS, the pressure coefficient of  $T_g$  is  $3.09 \times 10^{-7} \text{ K/Pa}$ ,<sup>65</sup> the isothermal compressibility,  $\kappa = 2.2 \times 10^{-10} \text{ Pa}^{-1}$ <sup>66</sup> and  $\rho = 1.04 \text{ g/cm}^3$ , yielding  $(\delta T_g / \delta \rho) = 1.35 \times 10^3 \text{ K/(g cm}^{-3})$ . To produce a 20 K drop in the  $T_g$  for a 10 nm thick film would require a density decrease of  $\sim 1.4\%$ . Such a large change in the average density of a thin film polymer has not been observed in experiment.<sup>53,67</sup> Thus, a reduced *average* film density cannot be used to explain the present observations. A mechanism focusing on changes at the interface between the polymer and the brush is more likely to be operative. Consider the following bilayer model for a film with thickness  $h$ : At the polymer-brush interface, the density of the polymer is  $\rho_i$  over a distance  $\zeta$  from the interface, but is  $\rho$ , the bulk density, for the remaining part,  $h - \zeta$  of the film. The  $T_g$  of the film as a whole would be given by  $T_g = T_g^{\text{bulk}} + (\delta T_g / \delta \rho)(\zeta/h)(\Delta \rho)$ , where  $\Delta \rho = \rho_i - \rho$ . For a 10 nm thick film, a 20 K reduction in  $T_g$  would be found when  $\zeta \Delta \rho \sim -1.48 \times 10^{-8} \text{ g/cm}^2$ . If we take  $\zeta = 3 \text{ nm}$ , several Kuhn lengths, then  $\Delta \rho / \rho = -0.05$ , i.e., a 5% density decrease at the interface. It should be remarked that  $\Delta \rho \zeta$  represents the surface excess (or surface deficit if  $\Delta \rho < 0$ ) of polymer segments at the substrate wall due to the polymer-substrate interactions. As  $h$  is increased, this effect diminishes according to  $\Delta \rho \zeta / h$  and explains the decreasing  $T_g$  reduction with increasing film thickness.

The foregoing discussion has focused on cases where the  $T_g$  decreases with decreasing film thickness. By considering favorable

interactions that make  $\Delta\rho$  positive, the same model can also describe systems with enhanced  $T_g$  with decreasing film thickness. Under the special condition where  $\Delta\rho = 0$ , the  $T_g$  of a film should remain the same as the bulk. This is the most closely fulfilled in this experiment with the  $f = 1$  brush. Previous theoretical estimate<sup>68</sup> shows that the interfacial energy for the  $f = 1$  sample would be small but finite  $\sim 0.1$  erg/cm<sup>2</sup>. The observed  $T_g$  with the  $f = 1$  brush (Fig. 8), being  $\sim 5$  K below the bulk  $T_g$ , is consistent with this estimate. This result shows that the effect of interfacial interaction on the  $T_g$  of polymer films cannot be formulated simply in terms of the polymer-substrate interfacial energy, but rather the surface excess,  $\Delta\rho\zeta$ , is more suitable. Recently, McCoy and Curro<sup>2,69</sup> estimated the surface excess of polystyrene sandwiched between confining walls that are non-wetting, neutral and strongly wetting, respectively, to the polymer, and found that the surface excess was negative in the first two cases, but positive in the last one. These estimates are in keeping with the present experimental and the ideas proposed thus far about the effect of the surface excess on the sign of the  $T_g$  shift.

In comparing our model with the  $T_g(h)$  reported by Keddie *et al.*,<sup>18,19</sup>  $\zeta\Delta\rho$  should be  $\sim 1/h^{1.8}$ . Confinement effect may give rise to strong perturbations to chain conformations.<sup>70,71</sup> However, the thickness at which changes in  $T_g$  start to occur ( $\sim 50$  nm for PS on SiO<sub>2</sub>), being bigger than the gyration radius of the polymer,  $R_g$  ( $\sim 15$  nm, here), would be too large to produce any noticeable effect. Computer simulation studies<sup>70,71</sup> show that perturbations to the segment density due to the interface persist over a distance,  $\xi_p > \sim R_g$ . Insofar, the estimates of the surface excess had been performed on polymer slabs with  $h \gg \xi_p$ . It would be interesting to estimate the surface excess for polymer slabs where this does not hold and see if it will demonstrate any thickness dependence. In particular, one would like to see if it will reproduce the  $1/h^{1.8}$  dependence deduced above.

### 3. A Major Issue

The fact that the  $T_g$  of polymer films deviates from the bulk value when the film thickness is decreased below a certain value suggests that

finite size effects of some sort must be involved. The biggest mystery about the problem of thin film  $T_g$  is the origin of such finite size effects. The onset of the  $T_g$  anomaly begins at a thickness that is surprisingly large ( $\sim 50$  nm for supported films and  $\sim 100$  nm for low- $M_w$  freely standing films) compared to the cooperativity size of glass transition, which is  $\approx 1-3$  nm.<sup>72,73</sup> At the same time, the molecular interactions at the interfaces – expected to be of the Lennard-Jones type because the polymers are apolar – are not long-range enough to provide a direct explanation either. While chain connectivity may account for the chain confinement effect noticed in the high- $M_w$  freely standing films (Fig. 4), it must not be relevant for the low- $M_w$  freely-standing films nor supported films since no  $M_w$  dependence was found in the  $T_g(h)$  dependence of these films. In particular, for supported PS films on Si, the absence of  $M_w$  dependence in  $T_g(h)$  was found for  $2.3 \leq M_w \leq 3000$  kDa,<sup>18,19,24,58</sup> corresponding to  $3.5 \leq R_{EE} \leq 128$  nm<sup>55</sup> that embraces very well the onset thickness of 50 nm for the finite size effect.

#### 4. Theoretical Models

There have been only a few models proposed to explain the  $T_g$  anomaly in polymer films, attributable to the fact that the physics of the glass transition is not very well understood.<sup>74</sup> In this section, I shall outline the ideas of these models. The interested readers are referred to the original papers for more details.

##### 4.1. Layered Model

The layered model discussed in Sec. 2 is the most popular and can be used to explain essentially all experimental observations. However, it is mostly phenomenological at this time and lacks any predictive power. For instance, the model by itself cannot predict the observed functional form of  $T_g(h)$  nor can it predict *a priori* whether the  $T_g$  of a polymer supported film should increase or decrease with respect to the bulk  $T_g$ . Nonetheless, it is often a good starting point for constructing further details to describe the data.<sup>18,19,25,54</sup>

#### 4.2. Sliding Chain Model

De Gennes<sup>75</sup> proposed the sliding chain model to explain the  $T_g$  reduction in freely-standing films. He suggested that it arose from the sliding motion of loops of polymer chains along their own contour. Only those loops with the two end points in contact with the polymer-air surfaces as shown in Fig. 9 were considered so that the barrier to the motion at the end points could be ignored. By taking into account the cooperativity size for such motion and arguing that it is those loops that are long enough to reach the mid-plane of the film that have the most influence on the  $T_g$  of the film, he arrived at a glass transition temperature,  $T_g(\text{slide})$ , that is linear in  $h$ . The glass transition temperature of the film would be determined by the sliding motion if  $T_g(\text{slide}) < T_g(\infty)$ . This condition occurs when the film thickness is smaller than a threshold value that is of the order of the end-to-end distance,  $R_{EE}$ , of the polymers. The model prediction provides a good description for the experimental result of the high- $M_w$  freely-standing films (Fig. 4). However, it does not predict a  $M_w$ -dependence in the slope of  $T_g(h)$  as observed in experiment nor does it predict a crossover from a high- $M_w$  to low- $M_w$  behavior (Fig. 4). The latter implies there to be an additional mechanism for the enhanced molecular mobility that competes with the sliding chain mechanism.

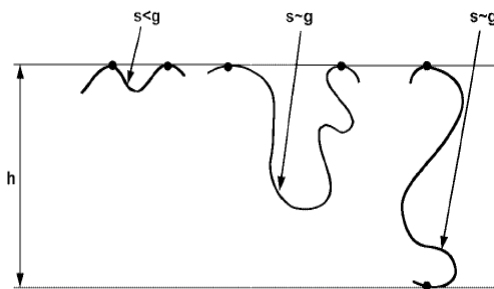


Fig. 9. Illustration of polymer loops with various loop lengths,  $s$ , sliding about the polymer-air surface. Only those loops with  $s \sim g \sim (h/a)^2$  and thus extend to the mid-plane of the film can have an impact on the  $T_g$  of the film. Figure was reproduced from Ref. 73, copyright EDP Sciences.

#### 4.3. Percolation Model

Long and co-worker<sup>76,77</sup> proposed a mechanism for the  $T_g$  reduction for apolar liquid films based on a percolation model for the glass transition. The idea is founded on spatial dynamic heterogeneity, *i.e.*, the presence

of spatially distributed domains with slow dynamics near the glass transition. In the percolation model, the glass transition occurs when the slow domains percolate through the sample. This condition defines the critical value  $\rho_c$  for the local mass density of a region above which the region is reckoned “slow”:

$$\int_{\rho_c}^{\infty} P(T, \rho) d\rho = p_c^{3D}, \quad (6)$$

where  $P(T, \rho)$  is the probability density distribution of the mass density  $\rho$  of the liquid at temperature  $T$ ;  $p_c^{3D}$  is the three-dimensional (3D) percolation threshold. (The exact value of  $p_c^{3D}$  depends on the form of the percolation network.) If the liquid is made to form a film, and the interactions between the liquid and the substrate are weak, the condition for glass transition would be modified to one requiring the slow domains to percolate in the plane. In the limit where the film thickness is smaller than the 3D percolation correlation length, the film is 2D and the percolation threshold on the RHS of Eq. 6 should be the 2D percolation threshold,  $p_c^{2D}$ . For an intermediate thickness  $h$ , the percolation threshold  $p_c(h)$  lies between  $p_c^{3D}$  and  $p_c^{2D}$ . Since  $p_c^{2D} > p_c^{3D}$  in general,  $p_c(h)$  increases and thereby  $T_g(h)$  decreases as  $h$  decreases. It can be shown that<sup>76</sup>

$$p_c(h) - p_c^{3D} \sim h^{-1/\mu}, \quad (7)$$

where  $\mu$  ( $\approx 0.88$  universally) is the critical exponent for the 3D percolation correlation length. By using Eq. 7 and assuming that  $P(T, \rho)$  is Gaussian and sharply peaked at the average mass density of the glass-forming liquid at temperature  $T$ , the authors<sup>76</sup> derived an expression for the  $T_g$  of the liquid confined in a film with thickness  $h$ :

$$T_g(h) \approx T_g(\text{bulk})[1 - (a/h)^{1/\mu}], \quad (8)$$

where  $a$  is, within a factor of order unity, equal to the monomer length. Clearly, the exponent given in Eq. 8,  $= 1/\mu = 1/0.88 = 1.136$  deviates from the value of  $\nu = 1.8$  (in Eq. 1) quoted above.<sup>18,19</sup> But as pointed out by several researchers,<sup>2</sup> the range of film thickness studied in experiment, which is usually 10 to 50 nm, is probably too small for the functional form of  $T_g(h)$  to be determined precisely. In fact, our group

had found  $\nu = 1.4$  for the same polymer film system.<sup>24</sup> Kim *et al.*<sup>78,79</sup> and Herminghaus *et al.*<sup>58,80</sup> even suggested a different function to describe  $T_g(h)$ , which is pertinent to the capillary wave model to be discussed next.

#### 4.4. Capillary Wave Model

In the capillary wave model proposed by Herminghaus,<sup>58,80</sup> a reduction in the  $T_g$  of polymer films can arise from the coupling of the viscoelastic surface capillary modes to the bulk of the film. Correspondingly, the thickness dependence of  $T_g$  is caused by the cut-off in the wavevector,  $q$ , of the surface capillary modes that varies as  $1/h$  – because only those modes with wavelengths longer than  $h$  can penetrate deep enough into the film to affect the  $T_g$ . With additional physical arguments,<sup>58</sup> Herminghaus simplified the relaxation rate of a film to:

$$\omega(q) \approx \frac{E}{\eta} + \frac{F(1)\gamma}{\eta} q, \quad (9)$$

where  $\gamma$  and  $E$  are the surface tension and elastic modulus of the polymer, respectively, and  $F(1)$  is a constant of order unity. By arguing that the memory kernel, which accounts for memory effects during relaxations of strains in the polymer, scales as  $1/T$  (where  $T$  is temperature), and applying the same criterion used in the mode-coupling framework for the transition of a system to be frozen into a non-ergodic state, Herminghaus arrived at the following relation for the  $T_g$  of thin films:

$$T_g(h) = T_g(\infty) \frac{a(0)}{\omega(h^{-1})} \quad (10a)$$

$$= T_g(\infty) \left(1 + \frac{h_0}{h}\right)^{-1}, \quad (10b)$$

where  $h_0 = F(1)\gamma/E \approx \gamma/E$  by Eq. 9. Kim *et al.*<sup>78</sup> showed that Eq. 10b could in fact also describe the data of Keddie *et al.* in Fig. 1 if

$h_0 = 0.68$  nm. Herminghaus *et al.*<sup>58</sup> found that Eq. 10b could describe their own data better than Eq. 1 if  $h_0$  was taken to be 0.82 nm. By putting  $\gamma = 31$  mN/m and  $h_0 = \gamma/E = 0.82$ , they obtained  $E \approx 44$  MPa, which corresponds to the value of  $E$  for PS in the middle of the glass transition on log scale.<sup>58</sup>

## 5. Dynamical Measurements of Polymer Films

The majority of dynamical studies of polymer films have measured the thickness dependence of  $T_g$ . Since all the models discussed above were constructed to give the  $T_g(h)$  dependence observed in experiment, more dynamical information about the films is needed to discriminate these models. Below I review the dynamical measurements made in the past on polymer films, and discuss any insights one may draw from those outcomes about the anomalous dynamics of polymer films.

### 5.1. Diffusion Experiments

Soon after the reduction of  $T_g$  was observed in polymer films, experiments were carried out to measure the diffusion rate (including tracer and inter-diffusion) in both supported polymer films<sup>81,82</sup> and later also freely-standing films.<sup>83,84</sup> In films showing a reduction of  $T_g$  with decreasing film thickness, only bulk-like or slower diffusion rates had been found. For example, in PS films supported by Si, the in-plane diffusion rate decreased monotonically with decreasing film thickness below  $h = 150$  nm.<sup>81</sup> In freely-standing PS films with  $M_w = 6900$  kDa, no thickness dependence was found for the out-of-plane diffusion rate down to a film thickness of 69 nm,<sup>84</sup> where there should be a  $T_g$  reduction of  $\sim 40$  K according to Fig. 4. This finding corresponds well with that of a holes growth measurement in freely-standing PS films (for  $51 \leq h \leq 91$  nm) where no significant growth of holes was observed until the temperature reached the bulk  $T_g$ .<sup>3</sup> Simple inference from these results would expect anything but a reduction of thin film  $T_g$ , which has caused some to query the interpretation of  $T_g$  reduction in those systems. It is recently pointed that the results on the thin film diffusion and  $T_g$

measurements can be reconciled: The higher mobility implied by the  $T_g$  reduction in polymer films is applicable only to motions on the segmental length scale; whole chain motions relevant to diffusion and growth of holes may not occur until temperatures reach the bulk  $T_g$ .<sup>3,4</sup> This picture was suggested<sup>3</sup> to be consistent with Semenov's analysis.<sup>85</sup>

## 5.2. Viscosity or Dynamical Mechanical Measurements

While the measured diffusion rate can be dominated by motions with length scales irrelevant to the glass transition, viscosity has traditionally been the dynamical quantity used to define  $T_g$ . In particular, glass transition is commonly described as a kinetic transition whereat the viscosity of a liquid increases by  $10^{13}$  times within a few degrees upon cooled across the glass transition temperature.<sup>86</sup> The information most often extracted from viscosity ( $\eta$ ) measurements is the functional dependence of  $\eta$  or relaxation time,  $\tau$ , on the temperature,  $T$ . For glass-formers in general, such dependences have been found to display the Vogel-Tammann-Fucher (VTF) scaling, which reads:

$$\tau(T) = \tau_0 \exp\left(\frac{U}{T - T_0}\right), \quad (11)$$

where  $\tau_0$  is the reciprocal attempt rate of molecular motion,  $U$  is related to the activation energy of the motion, and  $T_0$  is the Kauzmann or Vogel temperature.<sup>62</sup> From Eq. 11, it is clear that either a reduction in  $U$  or  $T_0$  would lead to a decrease in  $\tau$  and hence  $T_g$ . There have been numerous efforts to measure the  $\tau(T)$  relation for polymer films at different film thicknesses. But they are relatively scarce, attributable to the difficulty generally involved in detecting responses from a small sample. (*c.f.* For a  $1 \text{ cm}^2 \times 10 \text{ nm}$  film, the mass of the polymer is only  $\sim 1 \text{ }\mu\text{g}$ .) Three main kinds of techniques have been used for the measurement of  $\tau(T)$  although other techniques have been used as well.<sup>84,87,88</sup> They are atomic force microscopy (AFM),<sup>37-42</sup> ac dielectric (and capacitance) spectroscopy,<sup>89-95</sup> and x-ray photon correlation spectroscopy (XPCS).<sup>96-98</sup> I briefly discuss the status quo of each of them.

**Atomic Force Microscopy:** Dynamical studies employing AFM techniques generally probe the surface dynamics of the polymer.<sup>37-42</sup> Because of the large number of factors that can influence the measurements, the conclusion can often depend on the interpretation adopted for the data, which may explain the vastly different AFM results reported by different groups on polystyrene (PS). By using forced modulation microscopy (FMM), Kajiyama *et al.*<sup>36-38</sup> showed that the surface of PS was already in a viscoelastic state even at room temperature, provided  $M_n < \sim 30\text{K Da}$  or the polymer contains some  $M_n < 30\text{K Da}$  components. With monodispersed PS with  $M_n = 40\text{K Da}$ , Hammerschmidt *et al.*<sup>39</sup> observed a modest reduction in the surface  $T_g$  ( $< 10\text{ K}$ ) by friction force microscopy (FFM), which is consistent with Kajiyama's observations. On the other hand, Ge *et al.*<sup>40</sup> measured no change or a slight increase in the  $T_g$  of monodispersed supported PS with  $3\text{K} \leq M_w \leq 6.7\text{M Da}$  and freely-standing PS films with  $M_w = 697\text{K Da}$  and  $32 \leq h \leq 140\text{ nm}$  by using shear modulation force microscopy (SMFM). To understand these different results, one should take a closer look at the experimental details. In the FMM studies of Refs. 36-38 the AFM cantilever was driven into vertical vibration at a frequency of 4 kHz, the in-phase and quadrature responses of the tip (under an average load of 25 nN against the sample) were measured at room temperature and used to deduce the storage modulus and loss tangent of the sample. The researchers concluded the surface of a polymer to be rubbery at room temperature on the basis that the loss tangent was an order of magnitude larger than the corresponding values of the bulk. In SMFM,<sup>40</sup> which is similar to FMM in spirit, the cantilever was driven in sideway oscillations at 1.4 kHz; the resulting amplitude of the tip, under a constant load of  $\sim 12\text{ nN}$  in Ref. 39 and 25 nN in Ref. 40, was monitored as the temperature was swept from room temperature to above the bulk  $T_g$ . The  $T_g$  of the polymer was determined by drawing linear extrapolations from the low- and high-temperature asymptotes of the data and seeking the intersection. Since the response amplitude increases as the tip penetrates into the sample (as demonstrated by the creep data in Fig. 2 of Ref. 40), if a surface rubbery existed and expanded with increasing temperature, the  $T_g$  so measured could be dictated by the expansion of this surface layer. We have estimated<sup>41,42</sup> the indentation of

an AFM tip into the surface of a polymer near its glass-to-rubber transition by using the Johnson-Kendall-Roberts (JKR) model.<sup>99</sup> The estimated indentation at loading,  $\delta_{\text{load}}$ , is represented by the dashed line in Fig. 10. Assuming the surface rubbery layer to be 10 (or 20 nm) thick, the creep compliance of this layer only needs to be 3 (or 6) times of  $J(0)$  in order for the tip to penetrate through this rubbery layer. (Note that if we had used the more popular Hertz model<sup>100</sup> to estimate  $\delta_{\text{load}}$ , which ignores the tip-sample adhesion interaction, we would have overestimated the needed increase of the creep compliance to be  $\sim 150$  (or  $\sim 400$ ) times.) Since the creep compliance usually changes by several orders of magnitude across the glass transition, this estimate shows that we may expect an AFM tip to penetrate through the surface rubbery layer if it exists. In Fig. 11 is shown the  $T$  dependence of the thickness of the rubbery layer,  $\delta(T)$ , modeled by Keddie *et al.*,<sup>18,19</sup> *i.e.*,  $= \delta(1-T/T_g(\infty))^{-1/\nu}$  (see Sec. 2). The intercept obtained from asymptotic linear extrapolations at the two ends of this curve is very near  $T_g(\infty)$  (Fig. 11). Although the AFM response *vs.*  $T$  curve is strictly speaking different from this curve due to the finite creep rate for the tip to penetrate the rubbery layer, one may envision that the position of the intercept would still be very close to  $T_g(\infty)$  due to the theoretical divergence of the rubbery layer thereat. Given the vast number of recent experiments showing the surface dynamics of PS to be enhanced,<sup>29,44,45,49</sup> the scenario portrayed in Fig. 11 is probable.

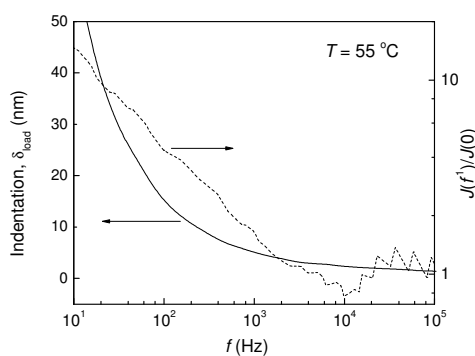


Fig. 10. Calculated tip indentation into a flat poly(*tert*-butyl acrylate) (PtBuA) ( $M_w = 148$  kDa,  $M_w/M_n = 17$ ,  $T_g = 50^\circ\text{C}$ ) plotted as a function of measurement probe rate,  $f$ . The data was obtained assuming the JKR model, and the radius of the AFM tip to be 50 nm, the applied force at loading to be 2.5 nN, and the adhesion data published in Refs. 41 and 42. The normalized creep compliance,  $J(f)/J(0)$  (dashed line; left scale) is also shown.

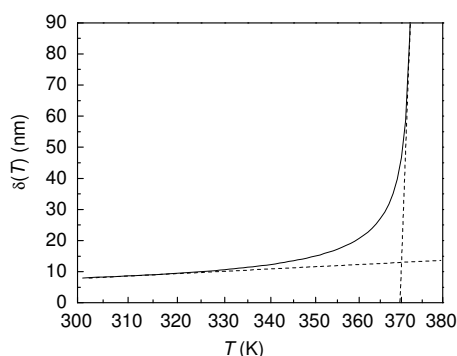


Fig. 11. Simulated temperature dependence of the thickness of the surface rubbery layer according to the model of Keddie *et al.*<sup>18,19</sup> discussed in Sec. 2.  $T_g(\infty)$  is 373 K here.

**Dielectric Spectroscopy:** Like AFM techniques, dielectric spectroscopy has been used in a large fraction of the dynamical measurements of polymer films, and produced some of the most elaborate data for  $\tau(T)$ . In this technique, the  $\tau(T)$  of a film is typically obtained by measuring the dielectric loss peak from a frequency (or temperature) scan at different temperatures (or frequencies). For PS films, it was found that when the film thickness was decreased, the dielectric loss peak broadened and at the same time shifted to higher frequencies or lower temperatures.<sup>89,90</sup> These results suggest that the dynamics in the film become more heterogeneous and at the same time more mobile on average. From the measured  $\tau(T)$ , the  $T_g$  reduction was found to be largely caused by a reduction of the Vogel temperature with decreasing film thickness.<sup>89,90</sup> But it is noteworthy that, except for Ref. 99, all dielectric measurements have been performed on polymer films sandwiched between metal electrodes as illustrated in Fig. 3(c). To make these films, the upper electrode was deposited onto the polymer film by thermal evaporation. Concerns have been raised on whether the evaporation process might alter the properties of the polymer film. In a recent experiment, Sharp *et al.*<sup>101</sup> fused two  $h/2$  thick supported films to make one  $h$  thick capped film. They found that the  $T_g$  of these films remained constant equal to  $T_g(\infty)$  for all thicknesses down to 8 nm, contrary to the results of previous dielectric measurements.<sup>89,90</sup> This result reaffirms the significance of a free surface to the reduction of  $T_g$  in polymer films, but at the same time casts doubts to the existing dielectric results, which had mostly been obtained from capped films.

**X-ray Photon Correlation Spectroscopy:** This is a state-of-the-art x-ray scattering technique in which a synchrotron x-ray beam is cut down to  $\sim 5^2$  to  $\sim 20^2 \mu\text{m}^2$  sizes to gain sufficient coherence in the beam so that a speckle pattern is produced upon scattering from a sample.<sup>96,102,103</sup> The relaxation time  $\tau$  of a polymer film is determined from the exponential decay of the intensity autocorrelation of the x-ray beam that is totally externally reflected from the film surface. According to Kim *et al.*,<sup>96</sup> this technique measures the dynamics in the top 10 nm of the film from the free surface. For PS films on Si,<sup>96</sup> the result from XPCS was found to display the relation,  $\tau(q_{||}) \sim Q(q_{||}h)/q_{||}$  (where  $q_{||}$  is the wave vector of the fluctuations on the film surface and  $Q(q_{||}h)$  is a function of  $q_{||}h$  only), which is consistent with the dynamic capillary wave theory and hence confirms that XPCS monitors the time variations in the surface structure of the film due to motions of the surface capillary waves. The smallest film thickness studied was 84 nm. The authors found no difference for the viscosity vs. temperature relation,  $\eta(T)$ , between the studied films and bulk PS.<sup>96</sup> By analyzing the dynamics of the surface capillary modes in a dynamically stratified film, the authors estimated that if the polymer film were composed of a 10 nm thick high-mobility surface layer with a viscosity 10 times smaller than the bulk value, resting on the remainder of the film that is “normal”, the total thickness of the film needs to be  $\sim 20$  nm in order for the effect to be reflected in the dynamics of the capillary waves.<sup>96</sup>

Several other studies have measured the viscosity of polymer films by analyzing the rate of growth of holes in the films.<sup>104-106</sup> In this method, the number density of holes increases rapidly with decreasing film thickness.<sup>107</sup> A high number density of holes causes the coalescence of holes at early times and thus prevents the opening of holes to be followed for an adequate amount of time.<sup>105,107</sup>

From the above brief overview of dynamical measurements of polymer thin films, we observe that the smallest thickness of films that have been studied for the viscosity is 27 nm by the hole-growth method.<sup>105</sup> As for  $\eta(T)$  measurements, the thinnest film that have been studied with no ambiguity is 84 nm by XPCS.<sup>96</sup> Clean measurements of  $\eta(T)$  in thin films with over the full thickness range of  $5 \text{ nm} < h < \sim 50 \text{ nm}$

are still lacking, which is necessary for making connections with the anomalous  $T_g$  observed in polymer film.

## 6. Concluding Remark and Outlook

In conclusion, the problem concerning the dynamics of polymers confined in thin films with thicknesses in the nanometer range is more than two decades old, and has become one of the most challenging current problems of polymer physics. Due to the widespread application of polymer films and the drastic thickness dependence of  $T_g$  that can sometimes take place, the issue is practical and has significant technological implications. One difficulty of the problem stems from the fact that most experiments had measured the glass transition temperature only, which, however, only represents one façade of the glass transition. To fully characterize the dynamical behavior would require the dynamical relaxation curve,  $\tau(T)$  to be measured for films with thicknesses where the  $T_g$  anomaly was observed, *i.e.*,  $5 \text{ nm} < h < \sim 50 \text{ nm}$  (Fig. 1). However, dynamical measurements of polymer films in the  $< 20 \text{ nm}$  thickness range are scarce, attributable to the small amount of polymer material ( $\sim 1 \mu\text{g}$ ) contained in these films. With the recent theoretical development, having the knowledge about the  $\tau(T)$  dependence of polymer films with thickness as such can be important: The capillary wave model discussed in Sec. 4.4 requires the free surface of the polymer film to be more mobile than the bulk since the fitted value of  $E \approx 44 \text{ MPa}$  corresponds to the value of a rubber. From the estimate of Kim *et al.*,<sup>96</sup> in order to see a reduced viscosity in the surface capillary modes due to a 10 nm thick mobile surface layer, one must examine films with thicknesses  $\leq 20 \text{ nm}$ . If the capillary wave model is operative, the  $\tau(T)$  function probed in a sufficiently thin film would be that of the surface layer and hence should demonstrate a much weaker temperature dependence than that of the bulk as in a rubber, but the absolute value of the relaxation time may depend on the film thickness as the coupling between the surface layer and the rest of the film may vary. On the other hand, if the percolation model is correct, the functional form of  $\tau(T)$  should vary continuously with decreasing film thickness as the system approaches the 2D limit with the high-temperature limit of the relaxation

time remaining the same for all thicknesses. The qualitatively different behaviors of  $\tau(T)$  of the two models should enable one to distinguish which model is at work. One should also mention the recent result of Fakhraai *et al.*<sup>108</sup> who measured the  $T_g$  of PS films on Si at different cooling rates, and found that the cooling rate vs.  $T_g$  followed the VTF scaling above bulk  $T_g$ , but became Arrhenius below it with the activation energy decreasing with decreasing film thickness. The former is consistent with a recent viscosity measurement of 18 nm PS films by time-resolved AFM.<sup>109</sup> If this behavior indeed reflects  $\tau^{-1}(T)$ , as tentatively suggested by the authors,<sup>108</sup> the physics of thin film  $T_g$  may require ideas different from the ones suggested so far. On the basis of the above discussions, obtaining a measurement of  $\tau(T)$  for films much thinner than 20 nm would be important for understanding the anomalous dynamics of polymer films. With the active pursuit of the problem by researchers around the globe, and new experiments with better approach and higher accuracy are designed, it is likely that new breakthroughs in the understanding of the problem will soon occur.

### Acknowledgements

The author would like to thank all the students, postdocs and colleagues who have worked and explored with her on this exciting area of polymer thin film dynamics. She also wants to thank the Polymer Division of NSF for supporting her research through the project DMR-0706096.

### References

1. M. Alcoutlabi and G. B. McKenna, *J. Phys. Condens. Matter*, 17, R461 (2005).
2. J. Baschnagel and F. Varnik, *J. Phys. Condens. Matter*, 17, R851 (2005).
3. C. B. Roth and J. R. Dutcher, *Soft Condensed Matters: Structure and Dynamics*. (Dekker, New York, 2004).
4. J. A. Forrest and K. Dalnoki-Veress, *Adv. Colloid Interface Sci.*, 94, 167 (2001).
5. G. Reiter, M. Hamieh, P. Damman, S. Slavovs, S. Gabriele, T. Vilmin and E. Raphael, *Nat. Mater.*, 4, 754 (2005).
6. G. Reiter and P.-G. de Gennes, *Eur. Phys. J. E*, 6, 25 (2001).
7. T. Kanaya, T. Miyazaki, H. Watanabe, K. Nishida, H. Yamano, S. Tasaki and B. Bucknall, *Polymer*, 44, 3769 (2003).
8. M. D. Morariu, E. Schaffer and U. Steiner, *Eur. Phys. J. E*, 12, 375 (2003).
9. C. Bollinne, S. Cuenot, B. Nysten and A. M. Jonas, *Eur. Phys. J. E*, 12, 389 (2003).

10. H. Zhao, Y. J. Wang and O. K. C. Tsui, *Langmuir*, 21, 5817 (2005).
11. O. K. C. Tsui, Y. J. Wang, H. Zhao and B. Du, *Eur. Phys. J. E*, 12, 417 (2003).
12. Y. J. Wang and O. K. C. Tsui, *Langmuir*, 22, 1959 (2006).
13. T. Miyazaki, K. Nishida and T. Kanaya, *Phys. Rev. E*, 69, 022801 (2004).
14. C. L. Jackson and G. B. McKenna, *J. Non-Cryst. Solids*, 131-133, 221 (1991).
15. G. Reiter, *Europhys. Lett.*, 23, 579 (1993).
16. G. Reiter, *Macromolecules*, 27, 3046 (1994).
17. G. Reiter, *Eur. Phys. J. E*, 8, 251 (2002).
18. J. L. Keddie, R. A. L. Jones and R. A. Cory, *Europhys. Lett.*, 27, 59 (1994).
19. J. L. Keddie, R. A. L. Jones and R. A. Cory, *Faraday Discuss.*, 98, 219 (1994).
20. J. H. van Zanten, W. E. Wallace and W.-L. Wu, *Phys. Rev. E*, 53, R2053 (1996).
21. W. E. Wallace, J. H. van Zanten and W.-L. Wu, *Phys. Rev. E*, 52, R3329 (1995).
22. L. Xie, G. B. DeMaggio, W. E. Frieze, J. DeVries, D. W. Gidley, H. A. Hristov and A. F. Yee, *Phys. Rev. Lett.*, 74, 4947 (1995).
23. J. A. Forrest and J. Mattsson, *Phys. Rev. E*, 61, R53 (2000).
24. O. K. C. Tsui and H. F. Zhang, *Macromolecules*, 34, 9139 (2001).
25. O. K. C. Tsui, T. P. Russell and C. Hawker, *Macromolecules*, 34, 5535 (2001).
26. A. M. Mayes, *Macromolecules*, 27, 3114 (1994).
27. H. Brown and T. P. Russell, *Macromolecules*, 29, 798 (1996).
28. T. Kajiyama, K. Tanaka and A. Takahara, *Macromolecules*, 28, 3482 (1995).
29. C. J. Ellison and M. Torkelson, *Nat. Mater.*, 2, 695 (2003).
30. F. Varnik, J. Baschnagel and K. Binder, *Phys. Rev. E*, 65, 021507 (2002).
31. P. Scheidler, W. Kob and K. Binder, *Eur. Phys. J. E*, 59, 701 (2002).
32. P. Scheidler, W. Kob and K. Binder, *J. Phys. Chem. B*, 108, 6673 (2004).
33. T. R. Bohme and J. J. de Pablo, *J. Chem. Phys.*, 116, 9939 (2002).
34. J. A. Torres, P. F. Nealey and J. J. De Pablo, *Phys. Rev. Lett.*, 85, 3221 (2000).
35. A. R. C. Baljon, M. H. M. van Weert, R. B. DeGraaff and R. Khare, *Macromolecules*, 38, 2391 (2005).
36. T. Kajiyama, K. Tanaka and A. Takahara, *Macromolecules*, 30, 280 (1997).
37. K. Tanaka, A. Taura, S.-R. Ge, A. Takahara and T. Kajiyama, *Macromolecules*, 29, 3040 (1996).
38. K. Tanaka, A. Takahara and T. Kajiyama, *Macromolecules*, 30, 6626 (1997).
39. J. A. Hammerschmidt, W. L. Gladfelter and G. Haugstade, *Macromolecules*, 32, 3360 (1999).
40. S. Ge, Y. Pu, W. Zhang, M. Rafailovich, J. Sokolov, C. Buenviaje, R. Buckmaster and R. M. Overney, *Phys. Rev. Lett.*, 85, 2340 (2000).
41. O. K. C. Tsui, X. P. Wang, J. Y. L. Ho, T. K. Ng and X. Xiao, *Macromolecules*, 33, 4198 (2000).
42. X. P. Wang, X. Xiao and O. K. C. Tsui, *Macromolecules*, 34, 4180 (2001).
43. Y. Liu, T. P. Russell, M. G. Samant, J. Stohr and H. Brown, *Macromolecules*, 30, 7768 (1997).
44. W. E. Wallace, D. A. Fischer, K. Efimenko, W.-L. Wu and J. Genzer, *Macromolecules*, 34, 5081 (2001).
45. Y. C. Jean, R. Zhang, H. Cao, J.-P. Yuan, C.-M. Huang, B. Nielsen and P. Asoka-Kumar, *Phys. Rev. B*, 56, R8459 (1997).
46. A. D. Schwab, D. M. G. Agra, J.-H. Kim, S. Kumar and A. Dhinojwala, *Macromolecules*, 33, 4903 (2000).

47. O. C. Tsang, F. Xie, O. K. C. Tsui, Z. Yang, J. Zhang, D. Shen and X. Yang, *J. Polym. Sci. B*, 39, 2906 (2001).
48. O. C. Tsang, O. K. C. Tsui and Z. Yang, *Phys. Rev. E*, 63, 061603 (2001).
49. T. Kerle, Z. Q. Lin, H. C. Kim and T. P. Russell, *Macromolecules*, 34, 3484 (2001).
50. M. Hamdorf and D. Johannsmann, *J. Chem. Phys.*, 112, 4262 (2000).
51. J. A. Forrest, K. Dalnoki-Veress, J. R. Stevens and J. R. Dutcher, *Phys. Rev. Lett.*, 77, 2002 (1996).
52. J. A. Forrest, K. Dalnoki-Veress and J. R. Dutcher, *Phys. Rev. E*, 56, 5705 (1997).
53. J. A. Forrest, K. Dalnoki-Veress and J. R. Dutcher, *Phys. Rev. E*, 58, 6109 (1998).
54. J. Mattsson, J. A. Forrest and L. Borjesson, *Phys. Rev. E*, 62, 5187 (2000).
55. K. Dalnoki-Veress, J. A. Forrest, C. Murray, C. Gigault and J. R. Dutcher, *Phys. Rev. E*, 62, 5187 (2001).
56. C. B. Roth and J. R. Dutcher, *Eur. Phys. J. E*, 12, 103 (2003).
57. C. B. Roth, A. Pound, S. W. Kamp and C. A. Murray, *Eur. Phys. J. E*, 20, 441 (2006).
58. S. Herminghaus, K. Jacobs and R. Seemann, *Eur. Phys. J. E*, 5, 531 (2001).
59. Pemra Doruker and Wayne L. Mattice, *J. Phys. Chem. B*, 103, 178 (1999).
60. T. G. Fox and P. J. Flory, *J. Appl. Phys.*, 21, 581 (1950).
61. A. Hariharan, S. Kumar and T. P. Russell, *J. Chem. Phys.*, 99, 4041 (1993).
62. G. Adam and J. H. Gibbs, *J. Chem. Phys.*, 43, 139 (1965).
63. P. G. Santangelo and C. M. Roland, *Macromolecules*, 31, 4581 (1998).
64. P. Mansky, Y. Liu, E. Huang, T. P. Russell and C. Hawker, *Science*, 275, 1458 (1997).
65. A. Eisenberg, *J. Phys. Chem.*, 67, 1333 (1963).
66. J. Brandrup and E. H. Immergut eds., *Polymer Handbook*, 3rd edn. (Wiley, New York, 1989).
67. W. E. Wallace, N. C. Beck-Tan and W.-L. Wu, *J. Chem. Phys.*, 108, 3798 (1998).
68. K. R. Shull, *Faraday Discuss.*, 98, 203 (1994).
69. John D. McCoy and John G. Curro, *J. Chem. Phys.*, 116, 9154 (2002).
70. I. Bitsanis and G. Hadziioannou, *J. Chem. Phys.*, 92, 3827 (1990).
71. J. Baschnagel and K. Binder, *Macromolecules*, 28, 6808 (1995).
72. U. Tracht, M. Wilhelm, A. Heuer, H. Feng, K. Schmidt-Rohr and H. W. Spiess, *Phys. Rev. Lett.*, 81, 2727 (1998).
73. M. T. Cicerone, F. R. Blackburn and M. D. Ediger, *Macromolecules*, 28, 8224 (1995).
74. P. W. Anderson, *Science*, 267, 1615 (1995).
75. P.-G. De Gennes, *Eur. Phys. J. E*, 2, 201 (2000).
76. D. Long and F. Lequeuz, *Eur. Phys. J. E*, 4, 371 (2001).
77. S. Merabia and D. Long, *Eur. Phys. J. E*, 9, 195 (2002).
78. J.-H. Kim, J. Jang and W.-C. Zin, *Langmuir*, 16, 4064 (2000).
79. J.-H. Kim, J. Jang and W.-C. Zin, *Langmuir*, 17, 2703 (2001).
80. S. Herminghaus, *Eur. Phys. J. E*, 8, 237 (2002).
81. B. Frank, A. P. Gast, T. P. Russell, H. Brown and C. Hawker, *Macromolecules*, 29, 6531 (1996).
82. X. Zheng, M. Rafailovich, J. Sokolov, Y. Strzhemechy and S. A. Schwarz, *Phys. Rev. Lett.*, 79, 241 (1997).
83. E. K. Lin, W.-L. Wu and S. K. Satija, *Macromolecules*, 30, 7224 (1997).

84. Y. Pu, H. White, M. Rafailovich, J. Sokolov, A. Patel, C. White, W.-L. Wu, V. Zaitsev and S. A. Schwarz, *Macromolecules*, 34, 8518 (2001).
85. A. N Semenov, *Phys. Rev. Lett.*, 80, 1908 (1998).
86. E. Donth, *The glass transition: relaxation dynamics in liquids and disordered materials*. (Springer-Verlag, Berlin, 2001).
87. C. Carelli, A. M. Higgins, R. A. L. Jones and M. Sferrazza, *Phys. Rev. E*, 73, 061804 (2006).
88. P. A. O'Connell and G. B. McKenna, *Science*, 307, 1760 (2005).
89. K. Fukao and Y. Miyamoto, *Phys. Rev. E*, 61, 1743 (2000).
90. K. Fukao and Y. Miyamoto, *Phys. Rev. E*, 64, 011803 (2001).
91. K. Fukao, S. Uno, Y. Miyamoto, A. Hoshino and H. Miyaji, *Phys. Rev. E*, 64, 051807 (2001).
92. K. Fukao, *Eur. Phys. J. E*, 12, 119 (2003).
93. L. Hatmann, W. Gorbatschow, J. Hauwede and F. Kremer, *Eur. Phys. J. E*, 8, 145 (2002).
94. A. Serghei and F. Kremer, *Phys. Rev. Lett.*, 91, 165702 (2003).
95. M. Wubbenhorst, C. A. Murray and J. R. Dutcher, *Eur. Phys. J. E*, 12, S109 (2003).
96. H. Kim, A. Ruhm, L. B. Lurio, J. K. Basu, J. Lal, D. Lumma, S. G. J. Mochrie and S. K. Sinha, *Phys. Rev. Lett.*, 90, 068302 (2003).
97. X. Hu, Z. Jiang, S. Narayanan, X. Jiao, A. R. Sandy, S. K. Sinha, L. B. Lurio and J. Lal, *Phys. Rev. E*, 74, R010602 (2006).
98. Z. Jiang, H. Kim, S. G. J. Mochrie, L. B. Lurio and S. K. Sinha, *Phys. Rev. E*, 74, 011603 (2006).
99. K. L. Johnson, K. Kendall and A. D. Roberts, *Proc. R. Soc. London A*, 324, 301 (1971).
100. H. Hertz, *J. Reine Angew. Math.*, 92, 156 (1882).
101. J. S. Sharp and J. A. Forrest, *Phys. Rev. Lett.*, 91, 235701 (2003).
102. O. K. C. Tsui and S. G. J. Mochrie, *Phys. Rev. E*, 57, 2030 (1998).
103. O. K. C. Tsui, S. G. J. Mochrie and L. E. Berman, *J. Synchrotron Rad.*, 5, 30 (1998).
104. K. Dalnoki-Veress, B. G. Nickel, C. Roth and J. R. Dutcher, *Phys. Rev. E*, 59, 2153 (1999).
105. J.-L. Masson and P. F. Green, *Phys. Rev. E*, 65, 031806 (2002).
106. C. Li, T. Koga, C. Li, J. Jiang, S. Sharma, S. Narayanan, L. B. Lurio, X. Hu, X. Jiao, S. K. Sinha, S. Billet, D. Sosnowik, H. Kim, J. Sokolov and M. Rafailovich, *Macromolecules*, 38, 5144 (2005).
107. G. Reiter, *Phys. Rev. Lett.*, 87, 186101 (2001).
108. Z. Fakhraai and J. A. Forrest, *Phys. Rev. Lett.*, 95, 025701 (2005).
109. O. K. C. Tsui, Y. J. Wang, F. K. Lee, C.-H. Lam and Z. Yang, *Macromolecules*, 41, 1465 (2008).